REPORT DOCUMENTATION PAGE	Form Approved OMB NO. 0704-0188

Public reporting burden for this collection of information is estimated to average 1 hour per response, including the time for reviewing instructions, searching existing data sources, gathering and maintaining the data needed, and completing and reviewing the collection of information. Send comment regarding this burden estimates or any other aspect of this collection of information, including suggestions for reducing this burden, to Washington Headquarters Services, Directorate for information Operations and Reports, 1215 Jefferson Davis Highway, Suite 1204, Arlington, VA 22202-4302, and to the Office of Management and Budget, Paperwork Reduction Project (0704-0188), Washington, DC 20503.

1. AGENCY USE ONLY (Leave blank)	2. REPORT DATE 4/30/00	3. REPORT TYPE AND DATES COVERED Final Technical Report 8/1/99-2/29/00

4. TITLE AND SUBTITLE	5. FUNDING NUMBERS
Development of TMI Logistic Fuel Solid Oxide Fuel Cell (SOFC) for Advanced Military Power Generation Systems	DAAD19-99-C-0035

6. AUTHOR(S)
Dr. Christopher Milliken, Mr. Michael A. Petrik, Dr. Robert C. Ruhl

7. PERFORMING ORGANIZATION NAMES(S) AND ADDRESS(ES)	8. PERFORMING ORGANIZATION REPORT NUMBER
Technology Management Inc. 9718 Lake Shore Blvd. Cleveland, OH 44108	

9. SPONSORING / MONITORING AGENCY NAME(S) AND ADDRESS(ES)	10. SPONSORING / MONITORING AGENCY REPORT NUMBER
U.S. Army Research Office P.O. Box 12211 Research Triangle Park, NC 27709-2211	ARO 40287.3-CH

12a. DISTRIBUTION / AVAILABILITY STATEMENT	12 b. DISTRIBUTION CODE
Approved for public release; distribution unlimited.	

13. ABSTRACT (Maximum 200 words)

Power generation systems based on the Technology Management, Inc. (TMI) solid oxide fuel cell (SOFC) are an optional modality for military applications requiring small scale, lightweight, compact sources of electrical power for extended missions. An example is a portable power generation system for battery recharging or replacement. Critical is the ability to insert this technology into existing military operations. This requires the ability to use military logistic fuel, preferably directly without pretreatment. Technology Management, Inc., has designed and is implementing a compact, integrated system using TMI's proprietary sulfur-tolerant planar solid oxide fuel cell (SOFC) and steam reformer, integrated into a compact unit which converts military logistic fuel into power directly and does not require either fuel pre-processing systems or fuel pretreatment.

14. SUBJECT TERMS		15. NUMBER IF PAGES
Solid Oxide Fuel Cell, SOFC, sulfur-tolerant, logistic fuel, syngas, portable, anode, cathode, electrolyte, catalyst, fuel efficiency, thermal cycling		29
		16. PRICE CODE

17. SECURITY CLASSIFICATION OR REPORT	18. SECURITY CLASSIFICATION OF THIS PAGE	19. SECURITY CLASSIFICATION OF ABSTRACT	20. LIMITATION OF ABSTRACT
UNCLASSIFIED	UNCLASSIFIED	UNCLASSIFIED	UL

Abstract

Power generation systems based on the Technology Management, Inc. (TMI) solid oxide fuel cell (SOFC) are an optional modality for military applications requiring small scale, lightweight, compact sources of electrical power for extended missions. An example is a portable power generation system for battery recharging or replacement. Critical is the ability to insert this technology into existing military operations. This requires the ability to use military logistic fuel, preferably directly without pretreatment. Technology Management, Inc., has designed and is implementing a compact, integrated system using TMI's proprietary sulfur-tolerant planar solid oxide fuel cell (SOFC) and steam reformer, integrated into a compact unit which converts military logistic fuel into power directly and does not require either fuel pre-processing systems or fuel pretreatment.

Key words
Solid Oxide Fuel Cell, SOFC, sulfur-tolerant, logistic fuel, syngas, portable, anode, cathode, electrolyte, catalyst, fuel efficiency, thermal cycling

Final Report

Development of TMI Logistic Fuel Solid Oxide Fuel Cells (SOFC) for Advanced Military Power Generation Systems

Contract number:	DAAD19-99-C-0035
Contractor Name:	Technology Management, Inc.
Contractor Address:	9718 Lake Shore Boulevard
	Cleveland, OH 44108
	Phone/Fax: 216-541-1000
	tmi@stratos.net
	(small business)

April 30, 2000

POC: Michael A. Petrik, Vice President
Ph: 216/586-5638 Fax: 216/586-3428

Table of Contents

Cover Page

List of Figures

List of Tables

1.0 Technical Summary

Technology Management, Inc. (TMI) has demonstrated in the laboratory a compact, power generator design which uses a novel solid oxide fuel cell (SOFC) running directly on military logistic fuel. Key to meeting the small size and light weight goals of a portable power generator (for battery recharging) were: i) the development of sulfur tolerant fuel reforming catalyst and sulfur tolerant anode electrodes to avoid the systems overhead required for sulfur removal and ii) the thermal and mechanical integration of the fuel reformer and stack assembly to reduce size and increase efficiency.

The current inventory of military power generation systems are combustion-based systems, and are generally noisy, polluting, inefficient, and limited to power outputs in the multi-kilowatt range. In comparison, TMI SOFC technology offers the potential for higher power densities and systems efficiencies, lower noise and emissions, and smaller system sizes. Functionally, the TMI SOFC fuel cells can extend mission length and serve applications at power ranges as low as 500 Watts operating on direct logistic fuel. The ultimate *long-term goal* for TMI is to produce a reliable, compact, lightweight, quiet, fuel efficient, military power source in the range of 300 to 500 watts which operates directly on military logistic fuel. Affordability is also an objective.

1.1 Overall Program Objective

The object of this program was to move toward the long-term goal by continuing to characterize and demonstrate the TMI Solid Oxide Fuel Cell (SOFC) stack, the most critical component, in an integrated laboratory test system. This program builds on advances and work completed under TMI's previous DARPA/ARO contract (DAAH04-94-C-0015). The specific areas of investigation of this program are outlined below.

Plan Tasks	Impact /Outcome
Reproducible Stack Demonstration	
Cathode Pressure Drop Reduction	Noise level, system efficiency
Stack Operating Parameters	Thermal cycling, start up, life
Fabrication and Quality Control Scale Up	Stack reproducibility, thermal cycling, efficiency, life
Seal-Separator Interface Improvement	Thermal cycling, life, physical ruggedness
Anode Interface Improvement	Life, thermal cycling, efficiency, performance, weight
Versatile System Development	
Air Flow Subsystems Engineering	Range of operating conditions, start up, stack thermal profile control → efficiency, life, performance
Overall Systems Design & Integration	Volume, weight, noise level, system efficiency, start up
Demonstration System Fabrication & Testing	Proof-of-concept

1.2 Summary of Achievements under Previous Contract

The goals of the SOFC development program under DARPA/ARO Contract Number DAAH04-94-C-0015 were to design and build a sulfur tolerant stack which could operate directly on logistic fuels (JP-8 with 0.3 wt% sulfur) and to package this stack into a compact, lightweight system.

Technology Management Inc.
9817 Lake Shore Blvd., Cleveland, Ohio 44108 - (216) 541-1000
Title: Development of TMI Logistic Fuel Solid Oxide Fuel Cells (SOFC) for Advanced Military Power Generation Systems – Final Report
Contract Number DAAD19-99-C-0035

April 30, 2000

Specific advances were made in several areas.

- Stability of cathode performance was improved by modifying firing conditions.
- Cell performance was tested and evaluated over a range of oxygen potential conditions in both anode and cathode.
- Thermally and mechanically integrated hot subassemblies were developed which demonstrated the use of hot exhaust from the stack to provide all the heat needed to operate the liquid fuel/water vaporizer and reformer.
- Thermal cycling of a 100 cell stack was demonstrated.

These tests and data significantly advanced the state of TMI stack technology toward the development of a practical solid oxide fuel cell generator operating on logistics fuels.

2.0 Background Information

Solid Oxide Fuel Cells (SOFCs) use an environmentally clean, electrochemical (non-combustion) process to generate electric power from a variety of fuels. A solid electrolyte operating at high temperature (800-$1000°C$) electrochemically converts gaseous fuels (hydrogen or mixed gases) and oxygen to electricity. Unlike polymer electrolyte membrane (PEM) fuel cells and alkaline fuel cells, SOFCs do not require electrolyte management (since electrolyte is solid), have very fast electrode kinetics, and can be configured into systems from under a kilowatt up to multi-megawatts. Further, the combination of high operating temperature and solid state operation means that the TMI SOFC stack assembly can be very reliable, compact, and noiseless. Systems can be designed to produce a high-grade heat by-product and high system efficiencies.

2.1 TMI SOFC Power Generation

Figure 1 shows an expanded schematic which illustrates the TMI SOFC single cell with conventional SOFC materials. Each cell is made up of four layers: (1) a fused, porous, reticulate cermet anode that provides both fuel gas distribution and electrical continuity; (2) a pre-sintered, non-porous, yttria-stabilized zirconia (YSZ) electrolyte for selective ion conduction; (3) a fused, porous, reticulate ceramic cathode (LSM) that provides air distribution and electrical continuity; and (4) a dense, high-temperature metallic alloy separator for bipolar electrical conduction from cell to cell.

The simplicity of the basic TMI cell design has advantages which impact cell and stack cost, systems part count and systems performance:

Figure 1. TMI SOFC Cell.

Use or disclosure of the data set forth above is subject to the restriction on the cover page of this report.

5

Technology Management Inc.
9817 Lake Shore Blvd., Cleveland, Ohio 44108 - (216) 541-1000
Title: Development of TMI Logistic Fuel Solid Oxide Fuel Cells (SOFC) for Advanced Military Power Generation Systems – Final Report
Contract Number DAAD19-99-C-0035

April 30, 2000

- The simple featureless, planar cell allows manufacture by commercially available fabrication equipment. Non-co-fired cell layers can be assembled into stacks using high volume, automated, low unit cost production equipment, a major requirement for success in commercial markets.

- The cell is tolerant of thermal cycling. The radial flow design has an unconstrained perimeter that accommodates dimension changes and minimizes the need for thermal expansion matching (a design constraint of other SOFC designs which limits the choice of materials).

- The mechanical stack assembly process allows for the immediate insertion of new or improved materials. Thus, materials can be chosen and optimized for performance characteristics, such as operation with sulfur-bearing fuels, including logistic fuels (JP-8).

- Air and fuel gas flows are supplied centrally through self-formed manifolds and exit through a unique radial flow pattern, which avoids the use of exhaust manifolds.

The primary advantage of a sulfur-tolerant system (which has *both* fuel reforming catalysts and fuel cells which are sulfur tolerant) is the avoidance of complex sulfur removal systems, and the operating procedures for recharging and disposing of the sulfur saturated waste. Sulfur tolerant systems require less systems components for direct operation on logistic fuels, which directly impacts system size, weight, and cost. Figure 2 shows a typical fuel-processing schematic comparison for the TMI SOFC system and typical polymer-electrolyte membrane (PEM) fuel cell system.

Under sponsorship by DARPA (Defense Advanced Research Projects Agency), TMI was one of the first companies to operate a complete sulfur-tolerant system (using an integrated steam reformer and stack) demonstrating operation of a total solid oxide fuel cell system operating on JP-8 fuel without sulfur-removal or fuel pretreatment.

Figure 2. Typical PEM vs. TMI SOFC Logistics Fuel Flowsheet.

Use or disclosure of the data set forth above is subject to the restriction on the cover page of this report.

6

Technology Management Inc.   April 30, 2000
9817 Lake Shore Blvd., Cleveland, Ohio 44108 - (216) 541-1000
Title: Development of TMI Logistic Fuel Solid Oxide Fuel Cells (SOFC) for Advanced Military Power Generation Systems – Final Report
Contract Number DAAD19-99-C-0035

Sulfur tolerance extends beyond logistic fuel and provides a competitive advantage in non-military markets by allowing the TMI system to use a wide variety of common fuels, particularly those containing sulfur contaminants, such as odorized natural gas, propane, kerosene and biogas.

3.0 Results of Task Work

3.1 Task 1. Cathode Pressure Drop Reduction:

Cathode pressure drop impacts the air flow requirements to the stack and the associated thermal system options and hardware requirements. With high cathode pressure drops, a compressor is required to supply air to the stack. A compressor is noisy, heavy, and consumes more power for operation than a blower, thereby potentially limiting the air-flow system options for a given system specification. A lower pressure drop allows the use of a lower weight, blower with lower noise levels. The current TMI cathode exhibits a pressure drop in the range of 4 to 6 psi. Use of a blower requires a pressure drop of approximately 1.0 psi.

A two step sequence was used to lower cathode pressure. The first requirement was to stabilize the microstructure. Then, geometric modifications were made to the cathode structure. Preliminary findings, along with supporting calculations, suggested physical flow channels can reduce pressure drops. Variables considered included channel geometry (depth, width, number of channels, etc.), and base material thickness and porosity.

Particle sintering in the cathode air distribution layer caused increasing air pressure drop over time. Reducing particle sintering within the component was necessary to achieve stable air flow characteristics. To reduce component sintering, several calcination conditions were evaluated for primary particle coarsening. Previous TMI cathode fabrication techniques used a high temperature process to produce large agglomerate powders for tape casting. In this process, the cathode particles were often quite large, 50-200 μm in diameter and the final air gas distribution layer thickness was over 500 μm. The present state-of-the-art requires a thinner layer thus an intermediate powder processing temperature was selected for coarsening trials. Intermediate temperatures were identified that significantly reduced particle coarsening. Time dependent back pressure increases went from 50-100% / 1000 hours to approximately 25-50% / 1000 hours.

A summary of cathode pressure drop reduction data based on the modified powder are shown in figures 3a and 3b. As shown in 3a, increasing effective channel dimension resulted in a pressure drop of approximately half in room temperature measurements. However, as shown in 3b, the composition and microstructure of the cathode was not sufficiently rigid to maintain such large channels for sustained high temperature operation. Based on calculations, the expected change in back pressure due only to gas viscosity effects predicts an increase in resistance of approximately 7:1. The actual increase was considerably higher, closer to 10:1 or 20:1 even in some cases. This supports the argument that channels collapse, at least partially, during operation. Coarsened cathode powder provided a lower increase in back pressure with time than the standard powder. Since the major gas conduction mechanism has been changed from porous

Use or disclosure of the data set forth above is subject to the restriction on the cover page of this report.

7

percolation to channeled flow, future work would focus on decreasing the porosity of the matrix to increase rigidity. This decrease is not expected to impact cell performance but should increase stability.

Figure 3. Summary of Cathode Pressure Drop Experiments
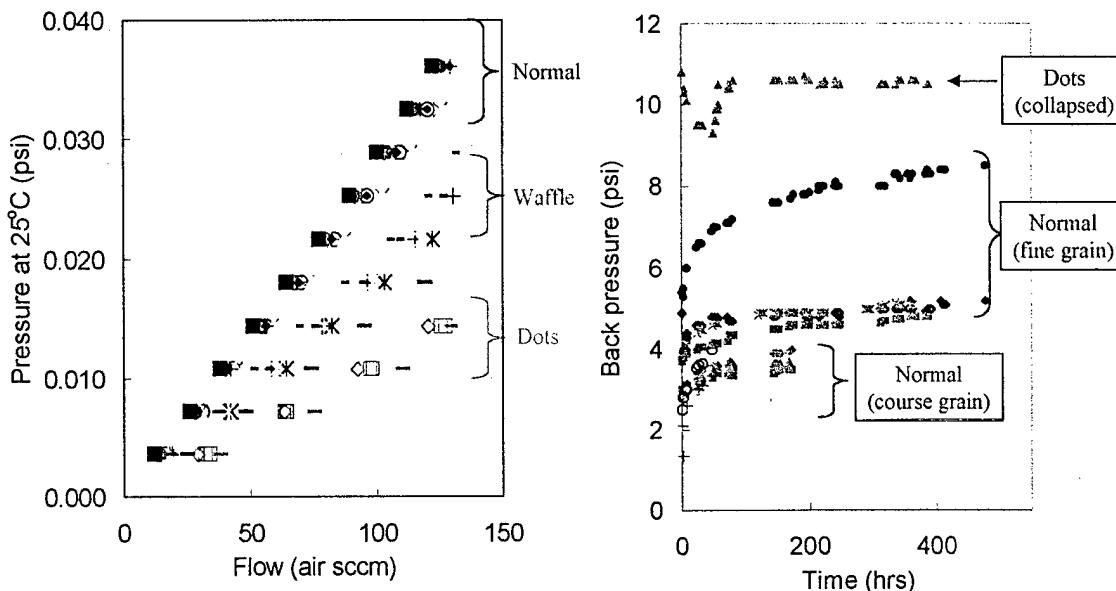
3.2   Task 2. Stack Operating Parameters:

All operational scenarios, except constant power, require a continuous balance among fuel, air, voltage, and current for stable, predictable operation. In addition to automatic controls, detailed start-up and/or operating procedures are essential to ensure stack and system performance, before introducing field variables such as mission length and actual operating conditions. An area of consideration is the operating range for cells, particularly the relationship between high fuel utilization on performance. Interfacial resistances dominate overall cell performance. Typical ohmic contributions for a self-supported YSZ cell are provided in Table 1. For normal materials at high temperatures, ohmic resistance contributes only a fraction of the total cell resistance. The remainder of the resistance is 'interfacial resistance' and includes both ohmic and non-ohmic behavior. This resistance is difficult to measure directly but a number of experiments have been conducted which suggest this resistance plays a substantial role in short and long term operation.

Table 1. Typical Ohmic Resistances for Common SOFC Materials.

Material	Conductivity $(\Omega*cm)^{-1}$ at 950°C	Thickness (microns)	Area Specific Resistance (Ωcm^2)
YSZ	0.1	300	3.0×10^{-1}
Metal Cermet*	100	50	5.0×10^{-5}
LSM*	25	50	2.0×10^{-4}
Separator	100	500	5.0×10^{-4}
Total			3.01×10^{-1}

* de-rated for low density

AC impedance is a useful technique but implementation and interpretation are difficult. The location of the working, counter, and reference electrodes can dramatically affect the observed response for essentially identical cells. A laboratory DC technique suggested by Dr. Harlan Anderson at the University of Missouri-Rolla utilizes embedded platinum electrodes in YSZ wafers. These tests measure the internal oxygen potential of the YSZ directly and isolate this value from the overall measurement. Tests using Dr. Anderson's wafers in the TMI cell configuration suggest that the majority of cell resistance occurs on the anode side of the cell. Those experimental findings lead to a focus on improving anode-cell and anode-separator interfacial characteristics. In addition, some experiments were still conducted on the cathode to categorically rule out polarization issues in that electrode. Results for one cell test summarized in Table 2 shows that gas phase polarization in the cathode does not affect cell performance. This was verified in two additional cell tests where equivalent cells were operated for nearly 1000 hours at different oxygen utilization conditions (from 1 stoic up to 5 stoics) with essentially no impact on performance (Figure 4). Target air flow for routine cell test qualifiers is 4.0 stoics.

Table 2. Impact of Cathode Oxygen Activity on Cell Performance

Total Cathode Gas Flow (sccm)	Cathode B.P. (psig)	pO_2 (atm)	Cell ASR (Ohm-cm^2)	Cathode Gas
277	6.0	0.293	*0.600*	House Air
60	2.0	1.136	*0.610*	Oxygen
120	3.6	0.635	*0.606*	Blend
283	7.7	0.328	*0.605*	Blend
279	7.7	0.328	*0.610*	Blend

Figure 4. Impact of Air Flow Rate on Cell Performance (125% to 25% of target).
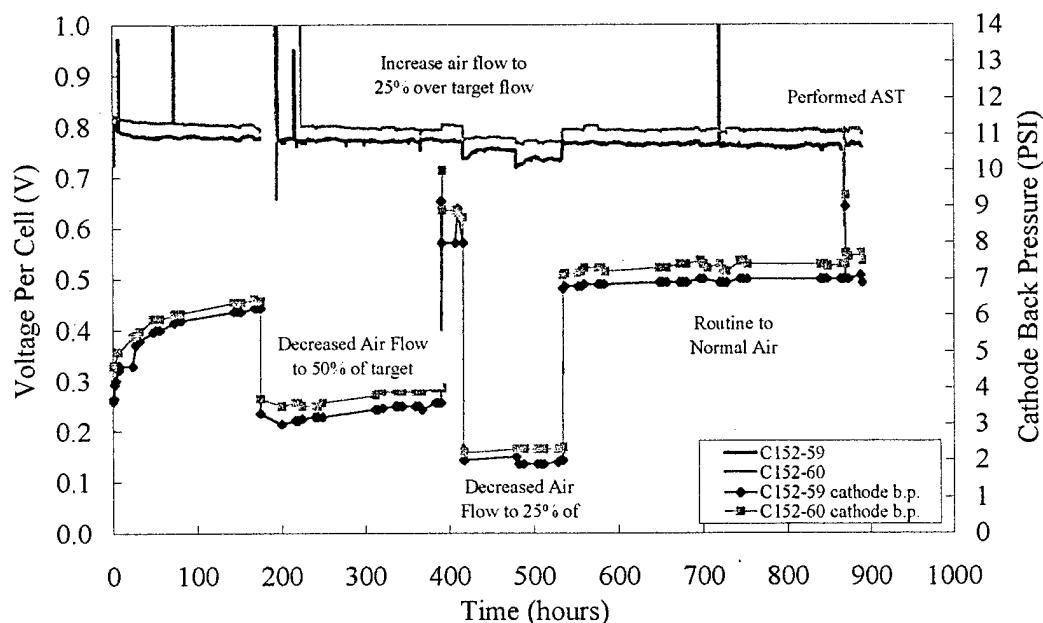
Characterizing the anode is challenging because of the relationship among parameters. The experimental controls are fuel flow rate and external resistance (which sets the total current). Cell voltage response is the observable factor. However, output voltage is not an intrinsic material property, but is related to cell resistance and Nernst potential. Nernst potential is in-turn related to flow and current and varies spatially on a cell. Three sets of experiments were conducted to attempt to resolve the interrelation of the parameters.

In the first experiment for the anode, fuel utilization was increased by decreasing gas flow rate at a constant current condition. In this case, ohmic resistances are constant and the only effects should be related to decrease in Nernst potential (due to utilization) and anode polarization effects (either adsorption or diffusional) . Results are shown in Figure 5. At fixed current density, the voltage drop across the cell (measured by comparing the observed voltage to the calculated Nernst potential at the lowest oxygen activity) increases with increasing fuel utilization. The increase is not dramatic but is beyond what might be explained by only considering decreasing Nernst potential.

Figure 5. Impact of Fuel Flow Rate on Cell Performance (H_2+6% H_2O, 194 mA/cm^2).
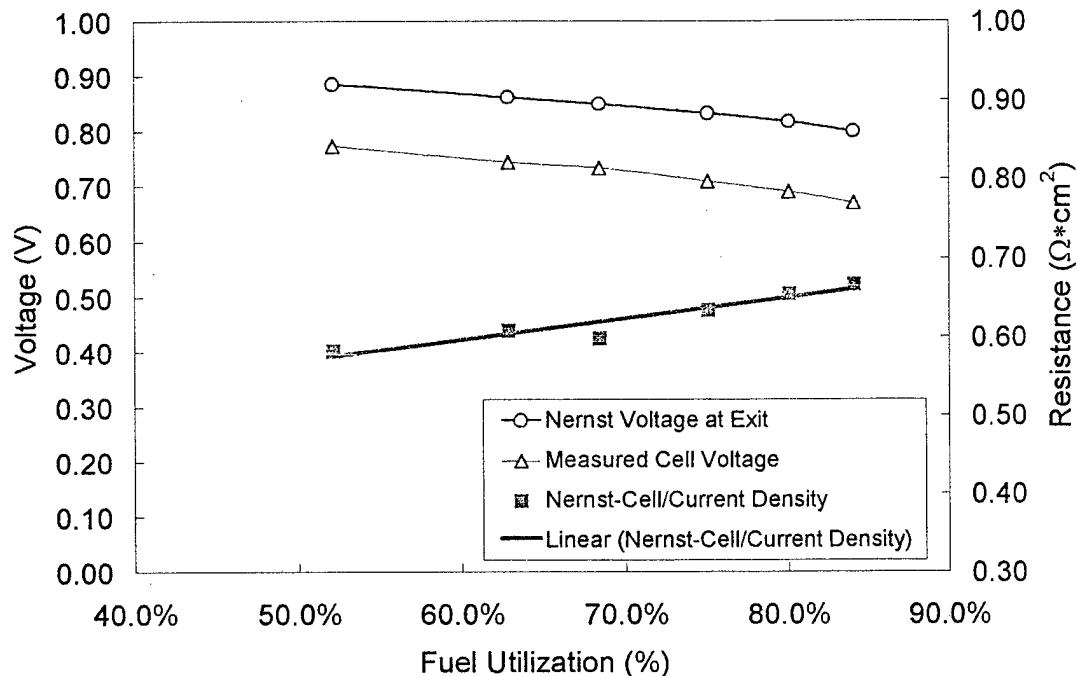
The second experiment involved running the same cell at a fixed fuel flow rate but with various current density conditions. This experiment concentrated on high utilization conditions where polarization was expected to be more substantial. The result is shown in Figure 6. In this case, the voltage would be expected to drop because of both the increased ohmic resistance of the cell and the decreased Nernst potential. However, the voltage drop due to ohmic resistance would be expected to be linearly changing if there are no electrode interactions. Since the ASR calculation is the slope of the voltage - current density curve, it should be a horizontal line as calculated herein. Because the slope already accounts for the instantaneous drop in Nernst potential (it is a ΔV calculation), the progressively increasing magnitude of resistance with increasing utilization agrees with the earlier result and suggests some additional non-ohmic mechanism at work.

The final experiment was run holding both the current and utilization constant and varying the fuel flow rate. A two-cell stack was run at a range of flow rates at constant utilization. This test was conducted using high inlet water conditions (affects the inlet Nernst Potential and spatial variation but not the exit composition) and is shown in Table 3. In this case, the cell performance at high flow conditions was better than would otherwise be expected looking only at the exit Nernst Potential (which is constant because overall utilization is constant). The area specific resistance (ASR) at the normal flow condition was slightly higher than an average stack but the trend is obvious nonetheless: stacks perform better at high flow conditions compared to low flow conditions assuming all other factors are held constant.

**Figure 6. Impact of Higher Utilization at Low Fuel Flow Conditions
using 6% humidified 25.7 cc H_2 + 25.7 cc N_2.**
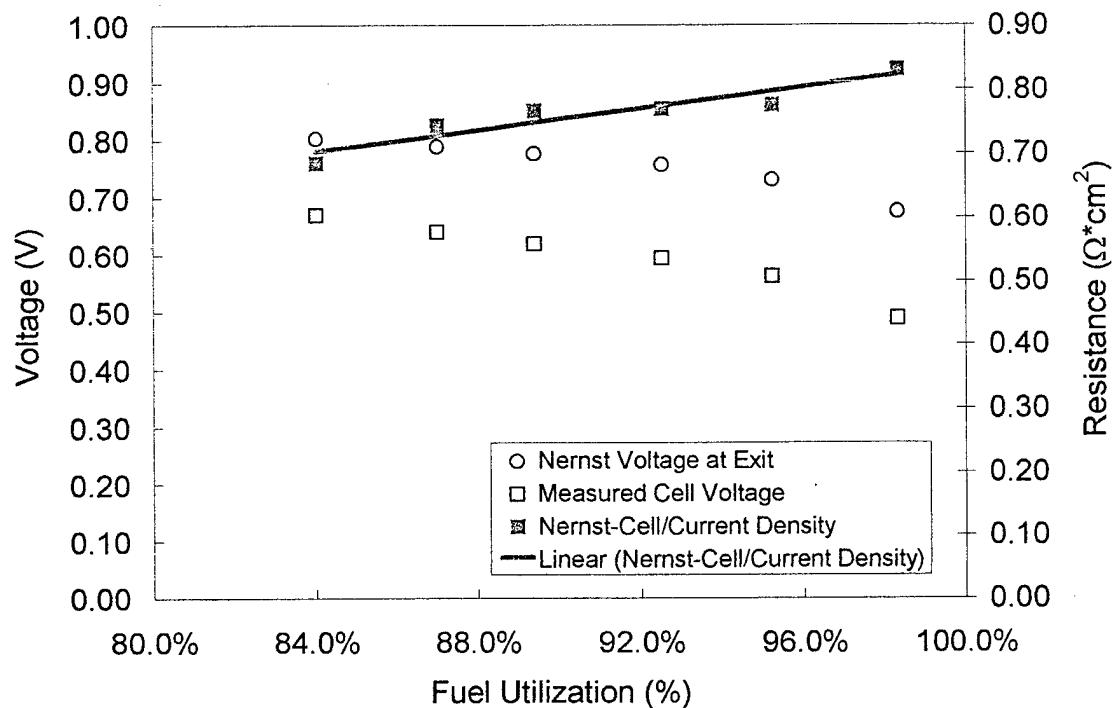
Table 3. Cell Performance at High Flow Conditions with Fixed Utilization (~60% FU)

H_2 Flow	H_2O Flow	Volts/Cell	Current Density (A/cm^2)	Nernst Potential	Nernst - Actual	(Nernst - Actual) / Current Density
20	23	0.691	0.086	0.887	0.197	*2.28*
40	42	0.682	0.172	0.887	0.205	*1.19*
50	51	0.659	0.216	0.887	0.229	*1.06*
60	59	0.627	0.259	0.887	0.261	*1.01*
80	74	0.562	0.345	0.887	0.325	*0.94*

There are a number of experimental complications with these experiments. The first is
determining resistance. There is a spatial variation in Nernst potential. First-pass resistance
calculations such as those shown in Figures 3 and 4 are estimates based on the minimum (exit)
Nernst potential. The second complication is determining the absolute active area. TMI has
found microscopic evidence in post test analysis of the high pO_2/low pO_2 transition region on the
cell, shown in Figure 7. The location of the transition region has been related to the flow
condition.

Figure 7. Microscopic Evidence of Transition Region.

The absolute determination of active area is therefore extremely challenging since it does not necessarily correspond to the geometric boundary of the electrode itself. Since cell resistance is normalized for active area, this factor could explain the variations in ASR in some of the experiments discussed above.

To compensate for experimental complications, TMI performs finite difference calculations on most cell tests. An example of these calculations are shown in the spreadsheet below in Table 4. This model calculates the instantaneous gas composition, voltage, and current density based upon 100 concentric radial volumes starting approximately at the inner diameter of the gas distribution electrode. Using this more complete analysis, there appears to be a non-ohmic increase in cell performance with increasing utilization above what might be expected from the Nernst potential suppression.

Several anode electrode models predict non-linear behavior. The first is a simple diffusion model. To remove oxygen from the anode surface, a hydrogen molecule (H_2) must be present at the surface at the same time. If the fuel gas is assumed ideal, the chance of any one gas molecule being a hydrogen molecule is equal to the concentration of hydrogen in the overall bulk gas. As utilization increases, the concentration of hydrogen decreases and the likelihood of the correct molecule encountering the surface decreases. "Diffusional limits" can become rate limiting for low hydrogen concentration values and for very thick anodes where gas diffusion paths are long (over 2000 microns) and not necessarily linear. In the TMI cell however, the complete anode thickness is only about 200 microns. Further, the gasses are completely exchanged within the cell in about 0.1 seconds (600 exchanges / minute). Given these parameters, bulk gas diffusional limits seem unlikely to be rate limiting.

Table 4. Finite Difference Cell Model for Determination of Cell Performance.

3/5/99 — Multipurpose Cell Model — 100 Steps
Data Entry Req'd on Humid — 884

Data Inputs

Item	Value	Units
Gaseous Fuel Flow	55.0	sccm
Added N2 Flow	50.0	sccm
Liquid Fuel Flow	0.00000	ml/min
Liquid Water Flow	0.0000	ml/min
Air Flow	290	sccm
Voltage	730	mV
Average ASR	0.912	Ohm-cm2
Center Temperature	950	C
Air Feed Pressure	5.00	psig
Electrolyte OD		mm
Electrode OD	54.55	mm
Center Inactive OD	13.22	mm
Air Oxygen	20.73	%
Air Leakage to Anode	0	sccm
Separator Conductivity	27.4	W/mC
Equiv. Sep. Thickness	0.50	mm
Cathode Coefficient	0.531	psi2/sccm
Feeds Heat Input	0.00	W
Reformer CO/CO2	1.40	

Gaseous Fuel Composition:

Species	Value	Units
H2	100.00	Mol %
H2O	0.00	Mol %
CO	0.00	Mol %
CO2	0.00	Mol %
CH4	0.00	Mol %
C2H6	0.00	Mol %
C3H8	0.00	Mol %
C4H10	0.00	Mol %
N2	0.00	Mol %
H2S	0.0000	Mol %
Total	100.00	

Liquid Fuel Data:

Item	Value	Units
H2 Content	14.00	Wt %
S Content	0.00	Wt %
Sp. Gr.	0.731	g/ml
LHV	43.3	MJ/kg

Calculated Values

Item	Value	Units
Power	2.977	W
Current	3.918	Amp
Cell Fuel Utilization	49.8	%
LHV Efficiency	30.1	%
Air Overall Stoic Ratio	2.12	
Net Power Density	149	mW/cm2
Net Current Density	196	mA/cm2
O/C Ratio		
Cell Rim Temp	940	C
Cell Rim Pressure	0.13	psig
Electrochemical Area	20.00	cm2
Cell Oxygen Utilization	23.5	%
Stoic Current	7.892	Amp
Max. Electrolyte Stress	5.1	MPa
Mean EMF	939	mV
HHV Efficiency	25.5	%
HHV	11.689	W
LHV	9.889	W

Reformed Fuel Gas

Item	Value	Units
Molecular Weight	14.497	g/mol
H2	50.91	Mol %
H2O	2.82	Mol %
CO	0.00	Mol %
CO2	0.00	Mol %
N2	46.28	Mol %
H2S	0.0	ppmv
CO+H2 (equiv)	50.91	Mol %
H2	55.00	sccm
H2O	3.04	sccm
CO	0.00	sccm
CO2	0.00	sccm
N2	50.00	sccm
H2S	0.0000	sccm
Total Flow	108.04	sccm
Liquid Fuel H/C	1.940	molar
Liquid Fuel Mass Flow	0.000000	g/min
Fuel LHV/HHV	0.846	
Total Water Vapor	3.0	sccm

Item	Value	Units
Cathode Air Flow	280.0	sccm
Cathode Air minus O2	221.8	sccm

Fuel Mixture Molar Flows

Species	Value	Units
C	0.000	sccm
H2	58.044	sccm
O	3.044	sccm
N2	0.000	sccm
S	0.00000	sccm

Radius mm	Fuel H2+CO	Air %O2	Anode O2(atm)	EMF mV	I mA/cm2	p mW/cm2	Radial q W	Temp C	Area cm2	Current mA	Air P psig
9.6	50.91	20.78	1.31E-18	1051	0	0	0.00	950	2.902	0	5.00
9.8	50.69	20.75	1.53E-18	1047	319	243	0.02	950	0.106	34	4.93
10.0	50.47	20.71	1.78E-18	1043	314	239	0.04	950	0.108	34	4.85
10.1	50.25	20.68	2.04E-18	1039	310	236	0.05	950	0.110	34	4.78
10.3	50.03	20.65	2.33E-18	1035	306	232	0.07	950	0.112	34	4.71
10.5	49.81	20.61	2.64E-18	1032	302	229	0.09	950	0.114	34	4.64
10.7	49.59	20.58	2.97E-18	1029	298	227	0.11	950	0.115	34	4.57
11.0	49.36	20.54	3.33E-18	1026	295	224	0.13	950	0.117	35	4.50
11.0	49.14	20.51	3.71E-18	1022	291	221	0.15	950	0.119	35	4.43
11.2	48.91	20.47	4.11E-18	1020	288	219	0.16	950	0.121	35	4.37
11.4	48.69	20.44	4.55E-18	1017	285	216	0.18	950	0.123	35	4.30
11.5	48.46	20.40	5.01E-18	1014	282	214	0.20	950	0.125	35	4.24
11.7	48.23	20.37	5.49E-18	1011	279	212	0.22	950	0.127	35	4.17
11.9	48.00	20.33	6.01E-18	1009	276	210	0.24	950	0.129	36	4.11
12.0	47.77	20.30	6.55E-18	1006	273	207	0.26	950	0.131	36	4.04
12.2	47.54	20.26	7.13E-18	1004	270	205	0.28	950	0.133	36	3.98
12.4	47.31	20.23	7.73E-18	1002	268	203	0.30	950	0.134	36	3.92
12.6	47.08	20.19	8.37E-18	999	265	201	0.32	950	0.136	36	3.86
12.7	46.84	20.15	9.05E-18	997	263	200	0.34	949	0.138	36	3.80
12.9	46.61	20.12	9.75E-18	995	260	198	0.35	949	0.140	36	3.74
13.1	46.37	20.08	1.05E-17	993	258	196	0.37	949	0.142	37	3.68
13.3	46.14	20.04	1.13E-17	991	256	194	0.39	949	0.144	37	3.62
13.4	45.90	20.01	1.21E-17	989	253	192	0.41	949	0.146	37	3.56
13.6	45.66	19.97	1.29E-17	987	251	191	0.43	949	0.148	37	3.51
13.8	45.42	19.93	1.38E-17	985	249	189	0.45	949	0.150	37	3.45
14.0	45.18	19.89	1.48E-17	983	247	188	0.47	949	0.152	37	3.39
14.1	44.93	19.86	1.57E-17	981	245	186	0.49	949	0.153	38	3.34
14.3	44.69	19.82	1.68E-17	979	243	184	0.51	949	0.155	38	3.28
14.5	44.45	19.78	1.78E-17	978	241	183	0.53	949	0.157	38	3.23
14.7	44.20	19.74	1.89E-17	976	239	181	0.55	949	0.159	38	3.17
14.8	43.96	19.70	2.01E-17	974	237	180	0.57	949	0.161	38	3.12
15.0	43.71	19.66	2.13E-17	972	235	178	0.59	949	0.163	38	3.07
15.2	43.46	19.63	2.25E-17	971	233	177	0.61	948	0.165	38	3.01
15.3	43.21	19.59	2.38E-17	969	231	176	0.64	948	0.167	39	2.96
15.5	42.96	19.55	2.52E-17	967	229	174	0.66	948	0.169	39	2.91
15.7	42.71	19.51	2.66E-17	966	227	173	0.68	948	0.171	39	2.86
15.9	42.46	19.47	2.80E-17	964	226	171	0.70	948	0.172	39	2.81
16.0	42.21	19.43	2.95E-17	963	224	170	0.72	948	0.174	39	2.76
16.2	41.96	19.39	3.11E-17	961	222	169	0.74	948	0.176	39	2.71
16.4	41.71	19.35	3.27E-17	959	220	167	0.76	948	0.178	39	2.66
16.6	41.45	19.31	3.44E-17	958	219	166	0.78	948	0.180	39	2.61
16.7	41.20	19.27	3.62E-17	956	217	165	0.80	948	0.182	39	2.56
16.9	40.94	19.23	3.80E-17	955	215	164	0.82	948	0.184	40	2.51
17.1	40.69	19.19	3.98E-17	953	214	162	0.84	947	0.186	40	2.46
17.3	40.43	19.15	4.18E-17	952	212	161	0.87	947	0.188	40	2.41
17.4	40.17	19.10	4.38E-17	951	211	160	0.89	947	0.190	40	2.36
17.6	39.91	19.06	4.59E-17	949	209	159	0.91	947	0.191	40	2.32
17.8	39.65	19.02	4.80E-17	948	207	158	0.93	947	0.193	40	2.27
18.0	39.40	18.98	5.03E-17	946	206	156	0.95	947	0.195	40	2.22
18.1	39.14	18.94	5.26E-17	945	204	155	0.97	947	0.197	40	2.18
18.3	38.88	18.90	5.50E-17	944	203	154	0.99	947	0.199	40	2.13
18.5	38.61	18.86	5.74E-17	942	201	153	1.02	947	0.201	40	2.09
18.7	38.35	18.81	6.00E-17	941	200	152	1.04	946	0.203	41	2.04
18.8	38.09	18.77	6.26E-17	939	198	151	1.06	946	0.205	41	1.99
19.0	37.83	18.73	6.53E-17	938	197	150	1.08	946	0.207	41	1.95
19.2	37.57	18.69	6.81E-17	937	195	148	1.10	946	0.209	41	1.91
19.3	37.30	18.65	7.10E-17	935	194	147	1.12	946	0.210	41	1.86
19.5	37.04	18.60	7.40E-17	934	192	146	1.15	946	0.212	41	1.82
19.7	36.78	18.56	7.71E-17	933	191	145	1.17	946	0.214	41	1.77
19.9	36.51	18.52	8.03E-17	932	190	144	1.19	946	0.216	41	1.73
20.0	36.25	18.47	8.36E-17	930	188	143	1.21	946	0.218	41	1.69
20.2	35.98	18.43	8.70E-17	929	187	142	1.23	945	0.220	41	1.64
20.4	35.72	18.39	9.05E-17	928	185	141	1.25	945	0.222	41	1.60
20.6	35.45	18.35	9.41E-17	927	184	140	1.28	945	0.224	41	1.56
20.7	35.19	18.30	9.78E-17	925	183	139	1.30	945	0.226	41	1.52
20.9	34.92	18.26	1.02E-16	924	181	138	1.32	945	0.228	41	1.47
21.1	34.65	18.22	1.06E-16	923	180	137	1.34	945	0.229	41	1.43
21.3	34.39	18.17	1.10E-16	922	179	136	1.36	945	0.231	41	1.39
21.4	34.12	18.13	1.14E-16	920	177	135	1.39	945	0.233	41	1.35
21.6	33.85	18.09	1.18E-16	919	176	134	1.41	944	0.235	41	1.31
21.8	33.59	18.04	1.23E-16	918	175	133	1.43	944	0.237	41	1.27
22.0	33.32	18.00	1.27E-16	917	173	132	1.45	944	0.239	41	1.23
22.1	33.05	17.95	1.32E-16	916	172	131	1.47	944	0.241	41	1.19
22.3	32.79	17.91	1.37E-16	914	171	130	1.50	944	0.243	41	1.15
22.5	32.52	17.87	1.42E-16	913	169	129	1.52	944	0.245	41	1.11
22.7	32.25	17.82	1.47E-16	912	168	128	1.54	944	0.247	41	1.07
22.8	31.98	17.78	1.53E-16	911	167	127	1.56	943	0.248	41	1.03
23.0	31.72	17.73	1.58E-16	910	165	126	1.58	943	0.250	41	0.99
23.2	31.45	17.69	1.64E-16	909	164	125	1.61	943	0.252	41	0.95
23.3	31.18	17.65	1.70E-16	907	163	124	1.63	943	0.254	41	0.91

The other possibility is chemical adsorption on the surface. Some researchers have postulated that an activated complex must be formed at the triple point boundary. Essentially, the H - O - H bonds must form on the surface along with a corresponding release of electrons. The rate of reaction is dictated by the amount of the adsorbed species (oxygen vacancy concentration combined with a mono-layer of hydrogen) and the ability of the surface to conduct electrons. In YSZ and in ceria, oxygen nonstoichiometry caused by gas phase equilibrium in the low pO_2 environment leads to an increase in vacancy concentration *and* an increase in electronic conductivity. The effect is particularly pronounced in ceria where the electronic conductivity can vary by six orders of magnitude. Essentially, the anode surface cannot effectively remove electrons as both local pO_2 and resistance increases.

TMI believes that the latter mechanism more effectively explains the small changes in performance that occur in addition to the change in driving potential. The most immediate remedy would be to dope the anode surface with elements that will impart electronic conductivity. In either case, the non-linear effect is small and operation > 75% fuel utilization is not an immediate short term objective. The decrease in performance is noted however and TMI understands that eventually, the issue will need to be considered.

3.3   Task 3. Fabrication and Quality Control issues:

Consistent stack manufacture is a necessary precursor to achieving acceptable life and stable performance required for engineering light weight, low volume systems capable of long missions. Variation in fuel distribution from cell to cell and on-cell both contribute to poor stability and can lead to catastrophic failure mechanisms.

One simple metric for considering the flow from cell to cell is to make an equivalent electrical circuit. In other words, a 100 cells connected to a common fuel plenum is equivalent to 100 resistors connected in parallel to a common wire. The pressure drop across the anode is equivalent to a voltage drop across a resistor, the gas flow through the bulk anode is equivalent to an electric current, and the back pressure is a measure of resistance. The flow through any one cell can be shown to be equal to:

$$F_{cell} = F_{total}\left(\frac{1}{(n-1)*X+1}\right) \qquad (1)$$

Where F_{cell} is worst-case fuel flow to one cell, F_{total} is the total fuel flow to the stack, n is the number of cells in the stack, and X is a figure of merit comparing the back pressure of one anode flowfield to another. For example, if the range of back pressure from one anode to another is 20%, then $X = 1.2$. In essence, X is also a measure of reproducibility. Fuel utilization per cell, flow and current are related to each other by:

$$FuelUtilization(\%) = 100 * \left(\frac{I*6.94}{FuelFlow(cc/min)}\right) \qquad (2)$$

where I is the electrical current (and hence ionic current through the electrolyte) and $FuelFlow$ is the fuel to that particular cell. Using these two equations, a relationship between fabrication reproducibility, X, and fuel utilization for the stack can be determined. The overall stack fuel utilization is simply:

$$StackFU(\%) = 100 * \left(\frac{I*n*6.94}{FuelFlow(cc/min)}\right) \qquad (3)$$

For example, using equation (3), a 100 cell stack operating at 4.0 amps total current per cell and 5.5 liters of H_2 fuel would be:

Use or disclosure of the data set forth above is subject to the restriction on the cover page of this report.

15

Technology Management Inc.

April 30, 2000

9817 Lake Shore Blvd., Cleveland, Ohio 44108 - (216) 541-1000

Title: Development of TMI Logistic Fuel Solid Oxide Fuel Cells (SOFC) for Advanced Military Power Generation Systems – Final Report

Contract Number DAAD19-99-C-0035

$$StackFU(\%) = 100 * \left(\frac{4*100*6.94}{5500}\right) = 50.5\% \qquad (4)$$

Using the same total fuel flow, current, and stack size and further assuming a variation an anode reproducibility of 30%, then the flow to the 'worst cell' in the stack (substitution into equation (1)):

$$F_{cell} = 5500\left(\frac{1}{(100-1)*1.30+1}\right) = 42.4 sccm \qquad (5)$$

From equation (2), 42.4 sccm flow to a cell with 4.0 amps of current per cell is a fuel utilization of 65.5%. So, although the average stack utilization is only 50.5%, somewhere in the stack, one cell is operating at a utilization of 65.5% (assuming the variation of 1.3).

TMI has found that running a cell in excess of 100% fuel utilization can lead to catastrophic delamination of the anode material. Assuming this boundary is reproducible, two operating regions can be mapped using overall stack utilization and common variations in anode back pressure. This graph is shown in Figure 8. To run a stack at high utilization conditions (above 75%) requires very consistent anode gas flow characteristics (below 30% variation).

Figure 8. Variation of Back Pressure and the Impact on Stack Reproducibility
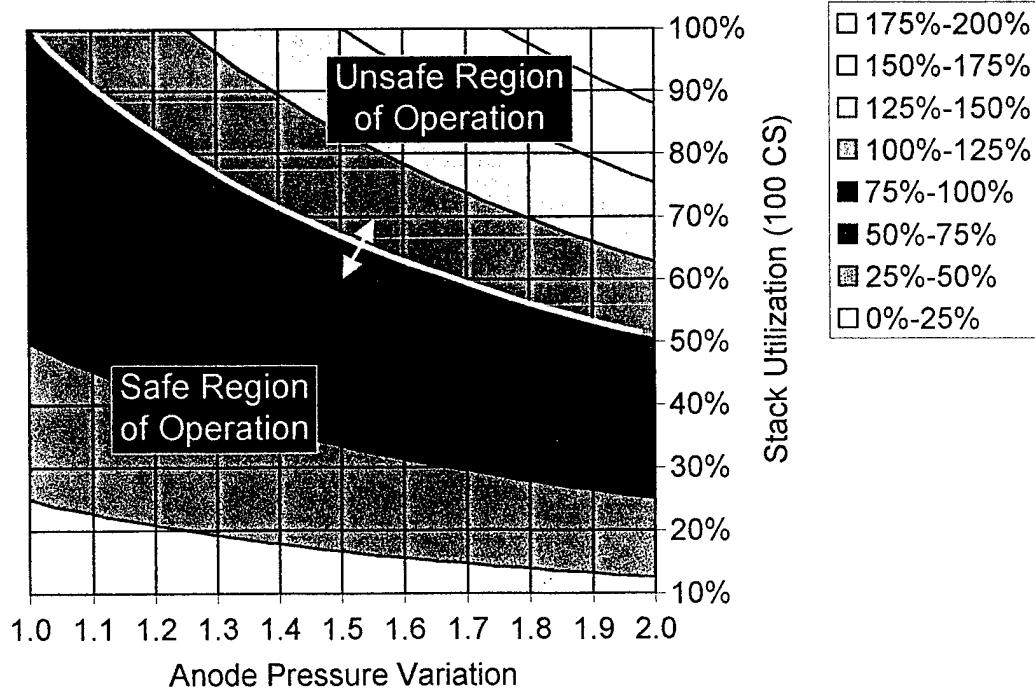
In the TMI case, the measurement in variation is easily determined (back pressure from cell to cell) but these particular calculations are geometrically unspecific. *They apply to any design where forced*

Use or disclosure of the data set forth above is subject to the restriction on the cover page of this report.

16

flow from a common manifold is used as the flow delivery mechanism. This describes the relationship among manufacturing capability, stack performance and catastrophic degradation.

Sealing integrity is critical to successful stack operation. Determining a robust sealing metric was one of the major advancement achieved during this program. Prior to June 1999, many stacks showed at least some leakage during start up. Poorly sealed stacks sometimes improved with time as the seal gaskets deform, closing pinhole leaks. Based on the analysis above, any leakage results in a local increase in fuel utilization (at a minimum) and can negatively impact life.

To address this issue, a full factorial analysis with replication was completed on seal sizing to explore the possibility of using thicker seals to provide improved integrity. The analysis examined two seal thickness specifications for the anode and two thickness specifications for the cathode. Since poor sealing occasionally occurred, selected size ranges were outside the range normally specified for stack tests. The results shown in Table 5 indicate that for all stacks (eight total), complete sealing could be achieved. Based on these tests, there was not a clear advantage to either range for either seal. All were comparable although the higher thickness appeared to be more consistent. No response was outside of the natural experimental variation window. Based on these results, the specification for seal dimension in large stacks was increased to a value within the ranges tested for both components. Stacks produced based on these changes have consistently showed excellent sealing with little air sensitivity.

Table 5. Full factorial analysis with replication for cathode and anode seal size.

	Anode Oversizing	Cathode Oversizing	Interaction	Output, 1st Test	Output, 2nd Test	Average	Range
	Low	Low	+	0.731	0.74	0.736	0.009
	High	Low	–	0.727	0.755	0.741	0.028
	Low	High	–	0.728	0.778	0.753	0.050
	High	High	+	0.773	0.761	0.767	0.012
SumAves+	1.51	1.52	1.50				
SumAves-	1.49	1.48	1.49				
Sum Aves	3.00	3.00	3.00				
Difference	0.02	0.04	0.01				
Effect	0.01	0.02	0.00				
d2	1.13						
N = n2^2	8		.				
Ave Sigma	0.09						
Sigma Effect	0.12						

3.4   Task 4. Seal-Separator Interfacial Improvements:

Thermal cycling caused by field operating conditions and mission requirements impact stack performance and seal integrity and must be anticipated. During a thermal cycle, the seal is the point of contact at which differences in thermal expansion coefficients between the separator and the electrolyte must be accommodated. Much of the thermal expansion stress is mitigated by TMI's radial design that allows a large degree of movement at the cell perimeter. Thermal cycling has been demonstrated on single cells at over 30 cycles without effect and promising

results have been shown in limited stack testing with one stack achieving nine thermal cycles. However, reproducibility has been an issue.

Several strategies were evaluated. The most successful was an oxide coated separator material. The first tests were conducted using three and five cell stacks under a number of conditions. Testing varied from 850-950°C on fuels including dry H_2, H_2+ 6% H_2O, H_2 + 6% H_2O + 300 ppm H_2S, as well as reformed fuels including steam reformed JP-8 and steam reformed CH_4. The stability at 950°C was less than desirable being 10-20% / 1000 hours on H_2 + 6% H_2O fuel. However, at 900°C, degradation rates were more acceptable at 2-5% / 1000 hours. The results of the best run including operation on the corrosive H_2 + 6% H_2O + 300 ppm H_2S, is shown in Figure 9. Higher water concentrations, found in reformed fuels, seemed to have some impact on stack performance and showed slightly higher decay rates. Thermal cycling data of small stacks with this separator is shown in Figure 10.

Several large stack tests completed included one 10-cell stack, two 25-cell stack tests and a 100-cell integrated stack test. The results of the second 25-cell stack is shown in Figure 11. This stack showed a relatively steep initial degradation. The rate was dependent upon temperature. Decreasing temperature reduced the degradation rate by approximately half. The stack was also subjected to three thermal cycles from operating temperature to approximately 100°C. The stack survived the deep cycles although the rate of decline in performance increased considerably after the third cycle. Nonetheless, the test was considered successful.

**Figure 9. Three Cell Stack at 200 mA/cm^2 at 900°C.**

Use or disclosure of the data set forth above is subject to the restriction on the cover page of this report.

18
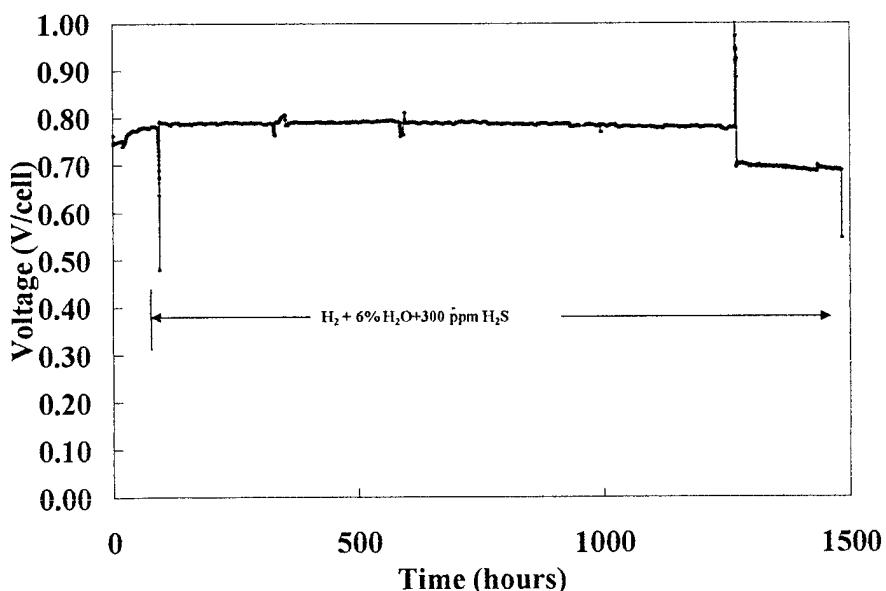
Figure 10. Three Cell Stack at 200 mA/cm² Cycled from 900°C.
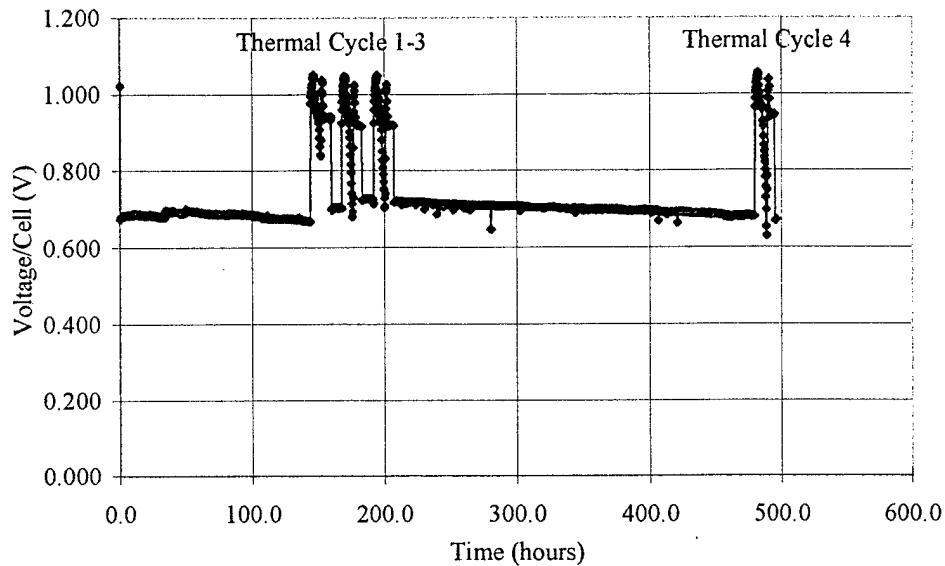
Figure 11. Twenty-five Cell Stack at 200 mA/cm² at ~900°C.

Use or disclosure of the data set forth above is subject to the restriction on the cover page of this report.

19
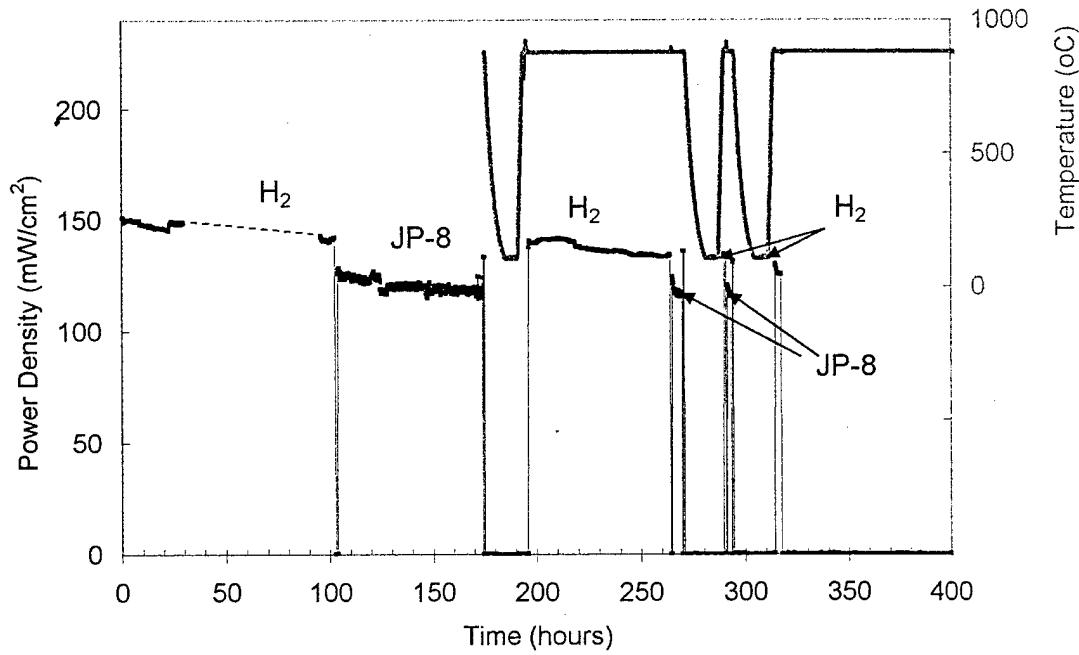
A 100 cell stack produced using the alternative separator material (summarized in Task 7 "Overall Integration" below) was thermally cycled repeatedly (discussed below) with no loss of performance. A 10 cell stack was similarly thermally cycled 15 times. Although fuel utilization could not be computed (the water vaporizer section had a fuel flow leak), the stack degraded only modestly during the test. Air-sensitivity checks made after each cycle showed no loss of sealing during the test.

3.5   Task 5. Anode Interfacial Improvements:

To achieve restartable, stable long-term stack performance, anode interface integrity is critical. The degree to which the anode interfacial integrity is challenged during operation, however, depends on start up and operation of the system (i.e., the operating conditions and mission requirements). Good electrode adhesion not only improves overall cell power density, but has a direct bearing on stack weight and volume.

Since successfully demonstrating sealing in large stacks in June 1999, TMI has started to evaluate other stack/system related problems. A major isolated issue is <u>catastrophic</u> degradation/failure of large stacks, defined as a rapid decrease in stack performance of >25% gross power output within 100 hours of operation. In some cases, the rates of decline are nearly precipitous but typically the decline is continuous and is not a 'step change'. Until complete sealing was achieved, catastrophic failures were attributed to broken cells, blown seals, etc. But other mechanisms influence these failures.

In 1999, TMI tested approximately 16 large 100-cell stacks and dozens of smaller size stacks. That work produced several compelling results. The first was that the fundamental materials set used by TMI for cell construction has intrinsic, desirable performance characteristics. TMI has reported to DARPA experiments on at least five multi-cell stack that achieved less than 4% / 1000 hour degradation rates on H_2/H_2O at 50% FU with the average degradation being 2-4%. Since these materials are of similar composition to those used by other SOFC developers (who have also reported good life characteristics), TMI believes that the fundamental fuel cell materials are adequate for near term development.

Many larger stacks, however, failed to achieved stable long term operation, even under H_2 fuel. Even tests that demonstrate stability often exhibited an initial decrease in performance before leveling out. This result is also not atypical of what has been reported in the open literature. Several SOFC developers including SOFCo, Ltd. and Z-Tek Inc., have publicly reported similar results with an initially rapid degradation followed by extended periods of stable operation. Because direct observation of cell components requires destruction of interfaces, determining the cause of this decay is very challenging.

In the TMI radial cell, where the components are less rigidly 'fused' together during fabrication, evaluation of the stacks after testing is easier. In the most recent tests, several stacks have come back from testing with literally only one cell in 50 showing any signs of severe degradation. Failed cells generally show extreme anode delamination. In addition, the cells show radial

delamination around the rim of the cell which does not appear to be related to any electrolyte cracking. This strongly suggests that gas distribution plays a dominant role. Data suggests that in many failed cells cracking seen in post-run analysis occurs either on cool down or during removal of the stack and that the cracks were not the origin of the failure. Often seals are intact in failed cells and do not exhibit direct oxidation patterns associated with seal leaks. Experimentally, the stack itself performed very well initially but degraded quickly.

The possibility that electrolyte breaking was causing a poor fuel distribution was considered. Dr. Arthur Heuer of Case Western Reserve was contacted to discuss the impact of cell breakage on degradation and poor performance. Dr. Heuer is an expert in YSZ fracture and the issue of how to improve cell robustness during operation was proposed. After some discussion, the methods to improve electrolyte strength focused on (1) eliminating defects in the raw components (2) reducing stresses during operation, (3) moving to a stronger 3 mol% Y_2O_3 material or, (4) incorporating Al_2O_3 into the YSZ. Alumina additions are done in some commercially available YSZ materials already (TOSOH, Inc. for example) based on the belief that it acts as a sink for other contaminants, particularly silica. All four options are being considered but represent long term development issues. After the consultation with Dr. Heuer, several experiments were conducted that showed that delamination could occur independent of cell breakage. YSZ failure will undeniably cause stack degradation but is not the inherent root cause of *all* failures.

TMI considered and evaluated the impact of gas distribution on cell performance at some length and a summary analysis was provided above. Clearly, poor distribution of reactants can lead to undesirable operational characteristics. Controls have been instituted to maximize reproducibility. Extensive quality control and fabrication improvements have been proposed (and are being implemented as resources permit). However, since quality control measures are inherently expensive and add cost to a final commercial product, even though this solution may eventually be successful, a more robust cell would be desirable.

Origin of Catastrophic Anode Delamination
One central area of interest is the relationship between the proposed failure mechanisms and the *magnitude* of the failure. A cell that is operated at beyond 100% utilization begins to consume power rather than produce it (relative to its neighboring cells). However, since a portion of the cell would still be in operation, the decrease in produced power would seem to be relatively minor. Cells have been tested in 'oxygen pumping' mode. The VI results of one cell are given in figure 12. The ASR in this case is approximately 8.5 $\Omega*cm^2$. This value is high but cannot explain the drop in stack performance. The decrease in stack performance is at least an order of magnitude beyond what this experiment suggests.

However, a gross delamination could explain large voltage drops seen in large stacks. Because of the poor contact area, a badly delaminated cell could easily act as a large resistance in the middle of the stack well beyond the materials limits.

Figure 12. Cell ASR in Reverse Polarized Mode.
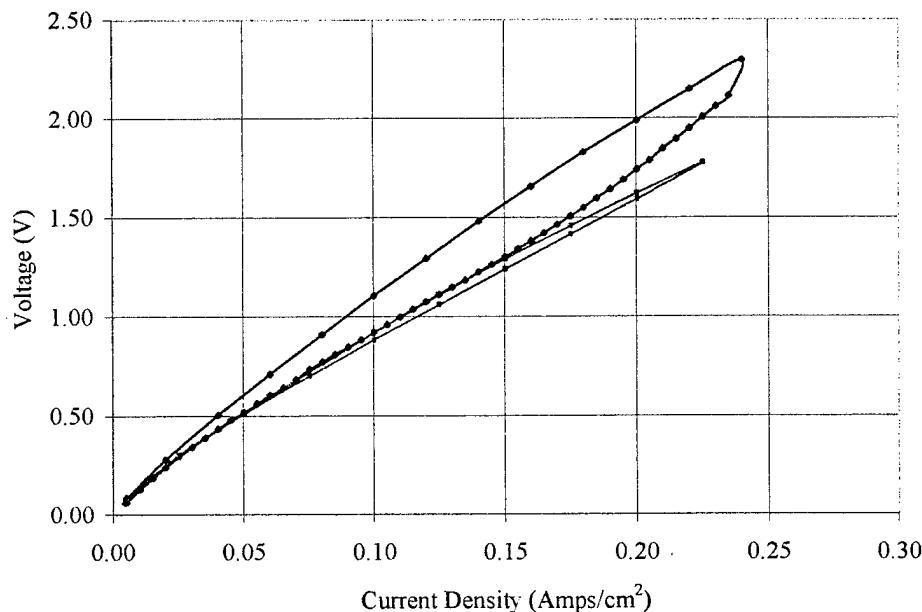
Tests were conducted to determine what conditions were necessary to cause complete delamination of the anode. Two identical cells were started for testing. Both tests were run for a short period to establish a performance baseline. In the first case, a cell was 'gas cycled' back and forth from fuel to air. This gas cycling exposed the cell to a number of stresses. Foremost is the change in anode density. For typical transition metal-cermets, the transition from metal (~ 9.0 g/cc density) to oxide (~6.0 g/cc density) results in a 50% increase in component volume. Linear dilatometry-type measurements suggest that there is little increase in thickness with oxidation so the increased volume must be accommodated by a decrease in porosity of approximately 10-15%. Similarly, the oxide part of the cermet also shows a slight volume increase of approximately 2-3%. Because the oxide in the anode is well bonded to the YSZ interface, this change might also be expected to introduce stresses. However, the cells can be returned to normal operation without negative affect.

The second cell was operated in 'reverse polarization' mode at 4.0 amps as shown in Figure 13. Essentially, within 24 hours, the voltage across the cell increased by over an order of magnitude. Post test evaluation showed massive delamination.

Figure 13. Cell ASR in Reverse Polarized Mode.
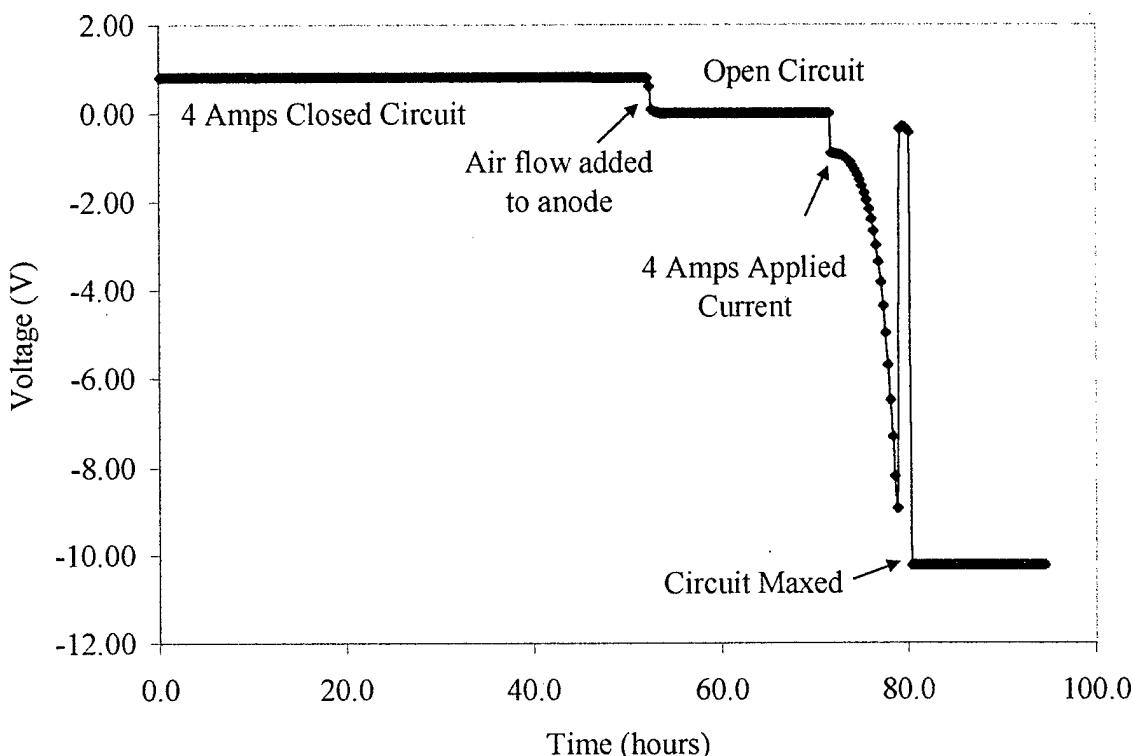
TMI has formulated a mechanism that may explain delamination, but is still investigating the implications. The transition state between an oxidized cell and a reduced cell offers a considerable range of possibilities including conduction mechanisms, reduced porosity, thermal stresses, etc. Experiments are planned to validate the hypothesis and results will be presented once they are conclusive.

3.6   Task 6. Air Flow Subsystems Engineering:

Air-flow management is a critical part of the control system needed to accommodate a broad range of system operating conditions while maintaining a consistent internal thermal profile for both stack and reformer. In addition to being fundamental to thermal management, air-flow subsystems not only supply oxygen to the stack but provide cooling for the stack. Calculations indicate that sufficient energy is available at the exhaust at a sufficiently useful temperature to provide all fuel processing. The challenge is re-distribution of that energy in both steady state and transient conditions.

The current system uses two air control circuits, one for condenser fan cooling, and a compressor-based system which, through a series of highly integrated heat exchange systems, provides cooling to the stack, oxygen for reaction, and heat to the reformer/vaporizer. Findings from operation of 100 cell stacks (300 W class) have shown that stack power, life, and efficiency

correlate to the thermal gradient in the hot subassembly. As expected, minimization of the temperature gradient within the stack and operation near 900°C produces good overall stack performance. The primary goal in the air flow subsystems engineering task was to design and incorporate a secondary air subsystem which improves stack cooling and overall system thermal control. The proposed strategy was to design a zoned air cooling system which uses an independent low pressure blower to provide additional cooling air to the stack.

After some additional measurements and calculations, a cooling scheme which allowed part of the air to bypass the stack was incorporated. TMI typically uses a very low air flow rate compared to other SOFC developers (typically less than 4.0 stoics) but even at this level, the stack only requires about 1/4th of the air flow for electrochemical purposes. An integral air-bypass was included in the hot-subassembly to allow approximately half of the air to bypass the stack and flow directly into the exhaust manifold. The bypass of hot gas provided better thermal equilibration overall without affecting the stack performance. Bypassing part of the cooling-air stream reduced the overall air back pressure through the system.

Figure 14 shows the profile of a stack running on hydrogen with the bypass. The five lines represent the profile radially around the inner hot assembly as well at along the length. The thermal gradient for the stack in this test was less than 60°C. This result has been demonstrated in other tests as well.

Figure 14. Integrated Laboratory Demonstration System Stack Thermal Profiles.

RUN NO. 99S135-09   HYDROGEN FUEL

10/22/99

Technology Management Inc.
9817 Lake Shore Blvd., Cleveland, Ohio 44108 - (216) 541-1000
Title: Development of TMI Logistic Fuel Solid Oxide Fuel Cells (SOFC) for Advanced Military Power Generation Systems – Final Report
Contract Number DAAD19-99-C-0035

April 30, 2000
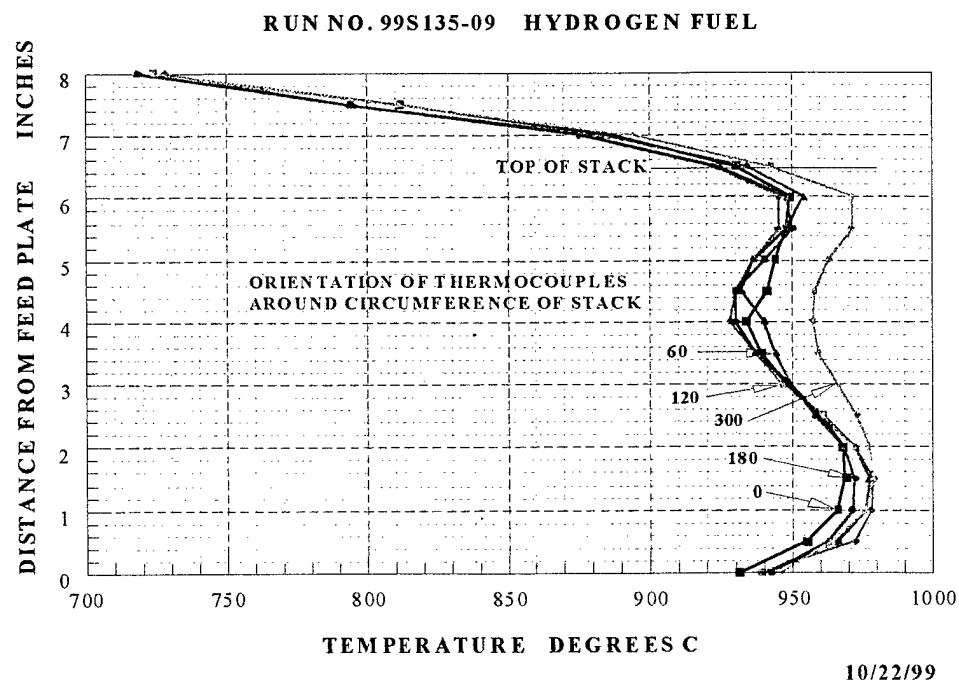
The air flow subsystems investigation shifted focus to the reformer/exhaust heat exchange zone in the hot subassembly. Initial experimental data indicated that near the middle of the reformer catalyst bed temperatures were lower than expected which increased the potential for coking. Causes for the lower temperature are either heat transfer limitations, excessive heat losses, or a combination of both.

3.7 Task 7. Overall Systems Design & Integration:

To the greatest degree possible, system designs were based on experience and development work from previous contracts and internal system designs. Under this task, the systems were augmented with additional instrumentation to measure more temperatures, pressures, and flows. Measurement devices were connected to computer data acquisition to allow more complete analysis of operation and to verify design performance. System design work included engineering calculations, bench top experiments, CAD designs, vendor and end user interactions, and prototype fabrication and testing. Engineering calculations consisted primarily of mechanical and electrical with materials and chemical engineering brought in as required.

3.8 Task 8. Demonstration System Fabrication & Testing:

Based on engineering and design work under Tasks 6 and 7 and stack development work under Tasks 1 through 5, system and stacks were fabricated and tested to verify that the stack technology was viable and that system concepts could be implemented which allow extended operation on JP-8 fuel with multiple system restarts from a cold condition (see Figure 15). A number of tests were completed from September to December. However, late in the program, an error was noted in the measurements of current. Some conditions vary slightly from what has traditionally been tested in benchmark tests.

Use or disclosure of the data set forth above is subject to the restriction on the cover page of this report.

25

Figure 15. Demonstration Test System
JP-8 Operating Configuration
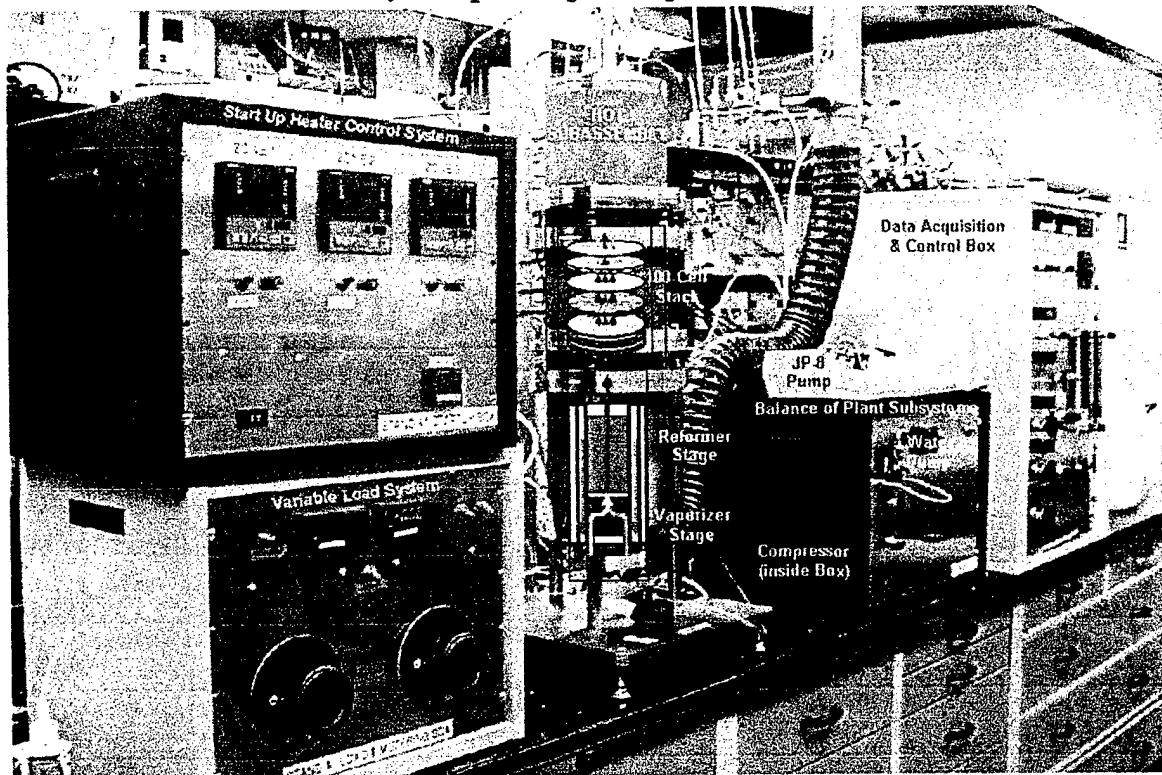
Two stacks in particular showed very encouraging results. A stack started in late October 1999 completed over 1000 hours of total operation as shown in Figure 16. The stack had excellent initial performance on both H_2 and JP-8. Coking events were identified (indicated by pressure increases) and *reversed* multiple times during the run by carefully changing fuel and water conditions. These 'decoking' conditions *removed carbon from the reformer but did not damage the stack.* After an initially steep degradation, the stack showed relatively stable performance. To examine longer stack operation on a reformed hydrocarbon fuel without the threat of coking, the stack was switched to methane and demonstrated stable, continuous stack performance (~240 Watts, ~30.0% LHV efficiency) for over 350 hours. Post run analysis of this stack showed excellent reduced anodes, except in one cell. This cell was badly delaminated and cracked, typical of a cell with poor fuel distribution and excessive fuel utilization. The nature of the cracks were such that positive determination of the order of events was not possible.

Figure 16. Large Stack Run 99S135-093 – Power and Pressure vs. Time
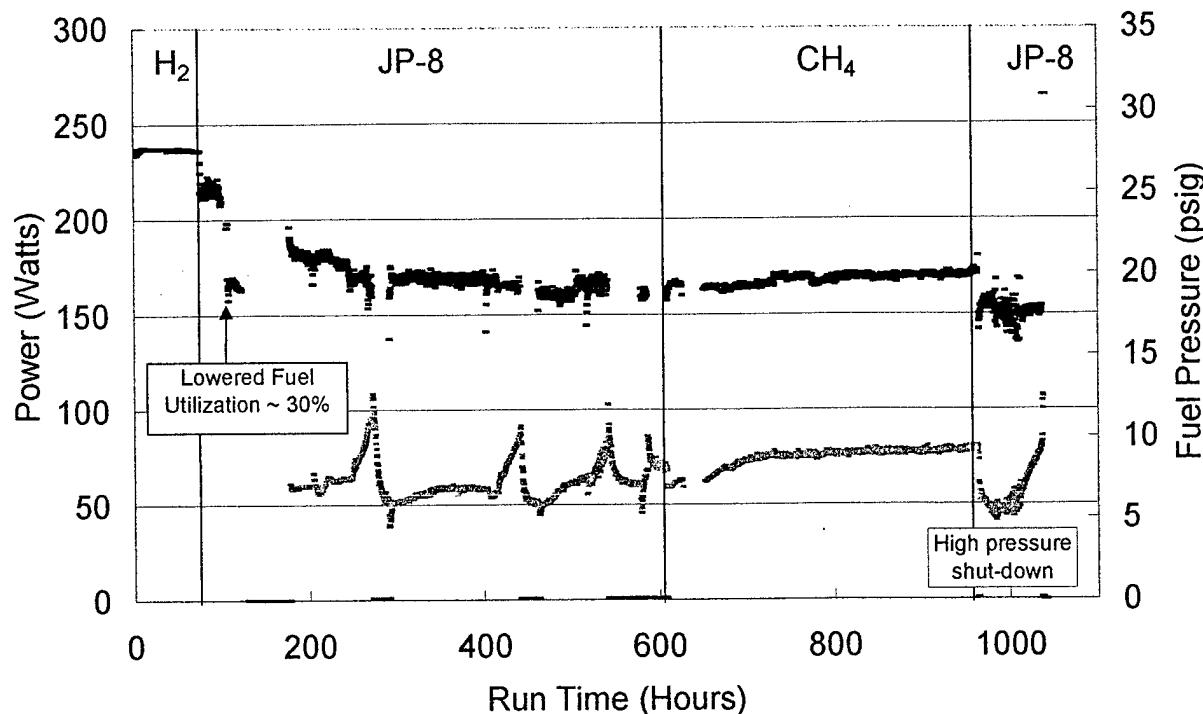
The other stack was started in late December 1999 using improved separator materials and an alternative anode geometry. As discussed in earlier reports and during the December DARPA site visit, fuel maldistribution from cell-to-cell in the stack and excessive fuel utilization in a few cells was theorized as a possible cause for electrode delamination, causing a dramatic loss of power in a relatively short time period (catastrophic degradation). To minimize the potential for this type of catastrophic degradation, the stack was initially operated at less than 50% overall fuel utilization and the performance tracked with time. Figure 18 shows no catastrophic degradation while operating on JP-8 fuel at fuel utilizations of approximately 37% and 44% for approximately 150 hours. As in previous runs, pressure increases caused by coking interrupted continuous operation, therefore the decision was made to thermally cycle the system after operating under de-coking conditions (to remove the carbon). The system successfully thermal cycled, with performance returning to approximately the same level (on JP-8). Continued pressure problems limited operation on JP-8, but under various conditions, the stack was thermally cycled three additional times, each with complete performance recovery and no sign of internal leaking.

To minimize the impact of coking on operation with hydrocarbon fuel, the stack was switched to natural gas after 420 hours, and operated at 60% fuel utilization. Under these conditions, the characteristic catastrophic degradation curve was observed and over 100 Watts of output lost. The stack was thermally cycled one time after this degradation and again performance returned.

Technology Management Inc.   **April 30, 2000**
9817 Lake Shore Blvd., Cleveland, Ohio 44108 - (216) 541-1000
Title: Development of TMI Logistic Fuel Solid Oxide Fuel Cells (SOFC) for Advanced Military Power Generation Systems – Final Report
Contract Number DAAD19-99-C-0035

The test was then terminated.

Figure 18. Thermally cycled 100-cell stack test.
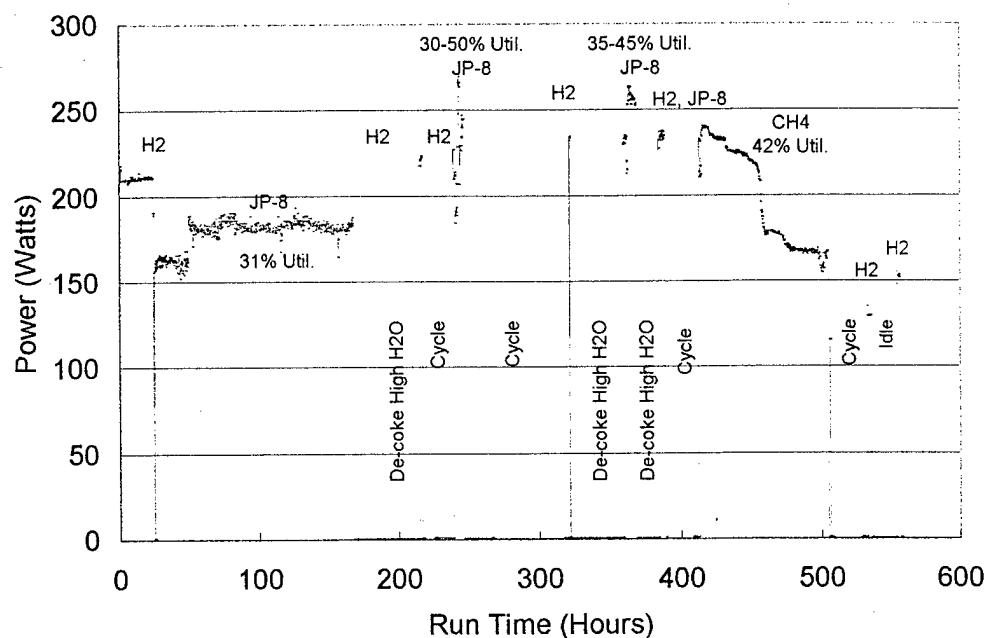
4.0 Conclusions

In general, the TMI SOFC technology continues to show promise for being able to operate directly on logistic fuels in small compact devices. Developments were made in fundamental materials of construction and methods of preparation to improve operational characteristics. Engineering calculations were performed and systems designs prepared to operate the TMI stack and catalyst in a compact, portable package. To the extent possible, application-specific systems were developed to accommodate stack requirements both geometrically (size, diameter, and shrinkage) and operationally (fuel and flow rate, vaporization and reforming, air handling, and thermal considerations). Testing of the laboratory demonstration system was conducted with the integrated stack/reformer operating with the balance-of-plant subsystems.

Thermal management becomes essential and critical at smaller sizes, particularly with respect to reforming heavier hydrocarbon fuels. Cell uniformity and reproducibility also play large roles in achieving higher efficiencies and stable long term performance. Other specific observations include:

1. Fundamental stack operation was reaffirmed on hydrogen and JP-8 fuels. Additional work has further characterized the mechanisms of long term degradation and thermal cycling and improved operation under these conditions.

2. Integration of the stack with TMI's closely coupled reformer design was validated at the 100 cell level. Thermal balance has been investigated and assumptions refined.

3. Thermal control concepts require additional refinement, particularly in the air flow and heat exchange systems.

These advances have significantly improved the capability of Technology Management, Inc. to develop an integrated solid oxide fuel cell generator operating on logistics fuels.

5.0 Recommendations for Future Work

There are three areas where additional research could significantly advance the technology toward a demonstration device.

First, solid oxide fuel cells (SOFCs) are power generation devices expected to operate over a wide range of operation conditions on a variety of reformed fuel products. The most critical feature to the Technology Management, Inc. SOFC system is a practical level of sulfur tolerance that allows fuel flexibility for a number of dual use applications. TMI has tested anode materials under a variety of conditions including on sulfur containing gasses (H_2 + 300 ppm H_2S in single cells and reformed JP-8 with 0.3 wt% S in stacks). However, anode materials have not been isolated and completely characterized on syngas representative of reformed JP-8, particularly at operating conditions which may be more representative of actual application operating conditions. To assure that scaled operation of a TMI prototype system in the field is an achievable goal, a program to characterize the most current cell design and materials under a range of syngas sulfur levels (up to reformed JP-8 with 0.3 wt% sulfur) and a range of operating conditions would be beneficial.

Second, stack development has clearly pointed toward fuel maldistribution as a critical step toward anode delamination and catastrophic stack failure. The mechanism of failure has been investigated and isolated to the conductive properties of the selected anode materials. A program to evaluate alternate materials that can survive wide variations in oxygen potential for prolonged periods without catastrophic failure would greatly enhance stack survivability and advance the solid oxide fuel cell community as a whole.

Finally, as Technology Management, Inc. has already demonstrated, the thermal integration of a small portable reactor operating on logistics fuel is a highly complex but resolvable issue. Additional effort directed at achieving better integration would be advantageous. This includes better measurements of thermal properties (i.e., effective conductivity of the insulation, hot sub assembly, catalyst support material, etc.) for the existing system of materials and additional measurements of dynamic system response such as that encountered during stop-start and transient load following conditions. Models have been developed that consider the interaction of these factors, but verification of these assumptions is necessary. To develop confidence and prognostication ability to scale up to multi-stack and multi-system hot swappable modules, testing these assumptions for validity is critical

Use or disclosure of the data set forth above is subject to the restriction on the cover page of this report.

29

REPORT OF INVENTIONS AND SUBCONTRACTS
(Pursuant to "Patent Rights" Contract Clause) (See Instructions on back)

The public reporting burden for this collection of information is estimated to average 1 hour per response, including the time for reviewing instructions, searching existing data sources, gathering and maintaining the data needed, and completing and reviewing the collection of information. Send comments regarding this burden estimate or any other aspect of this collection of information, including suggestions for reducing the burden, to Department of Defense, Washington Headquarters Services, Directorate for Information Operations and Reports (9000-0095), 1215 Jefferson Davis Highway, Suite 1204, Arlington, VA 22202-4302. Respondents should be aware that notwithstanding any other provision of law, no person shall be subject to any penalty for failing to comply with a collection of information if it does not display a currently valid OMB control number.

PLEASE DO NOT RETURN YOUR COMPLETED FORM TO THIS ADDRESS. RETURN COMPLETED FORM TO THE CONTRACTING OFFICER.

1.a. NAME OF CONTRACTOR/SUBCONTRACTOR	c. CONTRACT NUMBER	2.a. NAME OF GOVERNMENT PRIME CONTRACTOR	c. CONTRACT NUMBER	3. TYPE OF REPORT (X one)
Technology Management Inc.	DAAD19-99-C-035			a. INTERIM / b. FINAL

b. ADDRESS (Include ZIP Code)	d. AWARD DATE (YYYYMMDD)	b. ADDRESS (Include ZIP Code)	d. AWARD DATE (YYYYMMDD)	4. REPORTING PERIOD (YYYYMMDD)
9718 Lake Shore Blvd. Cleveland, OH 44108	8/1/99			a. FROM 8/1/99 b. TO 2/29/00

SECTION I - SUBJECT INVENTIONS

5. "SUBJECT INVENTIONS" REQUIRED TO BE REPORTED BY CONTRACTOR/SUBCONTRACTOR (If "None," so state)

NAME(S) OF INVENTOR(S) (Last, First, Middle Initial) a.	TITLE OF INVENTION(S) b.	DISCLOSURE NUMBER, PATENT APPLICATION SERIAL NUMBER OR PATENT NUMBER c.	ELECTION TO FILE PATENT APPLICATIONS (X) d.				CONFIRMATORY INSTRUMENT OR ASSIGNMENT FORWARDED TO CONTRACTING OFFICER (X) e.	
			(1) UNITED STATES		(2) FOREIGN		(a) YES	(b) NO
			(a) YES	(b) NO	(a) YES	(b) NO		
None								

f. EMPLOYER OF INVENTOR(S) NOT EMPLOYED BY CONTRACTOR/SUBCONTRACTOR

(1) (a) NAME OF INVENTOR (Last, First, Middle Initial)	(2) (a) NAME OF INVENTOR (Last, First, Middle Initial)	g. ELECTED FOREIGN COUNTRIES IN WHICH A PATENT APPLICATION WILL BE FILED	
(b) NAME OF EMPLOYER	(b) NAME OF EMPLOYER	(1) TITLE OF INVENTION	(2) FOREIGN COUNTRIES OF PATENT APPLICATION
(c) ADDRESS OF EMPLOYER (Include ZIP Code)	(c) ADDRESS OF EMPLOYER (Include ZIP Code)		

SECTION II - SUBCONTRACTS (Containing a "Patent Rights" clause)

6. SUBCONTRACTS AWARDED BY CONTRACTOR/SUBCONTRACTOR (If "None," so state)

NAME OF SUBCONTRACTOR(S) a.	ADDRESS (Include ZIP Code) b.	SUBCONTRACT NUMBER(S) c.	FAR "PATENT RIGHTS" d.		DESCRIPTION OF WORK TO BE PERFORMED UNDER SUBCONTRACT(S) e.	SUBCONTRACT DATES (YYYYMMDD) f.	
			(1) CLAUSE NUMBER	(2) DATE (YYYYMM)		(1) AWARD	(2) ESTIMATED COMPLETION

SECTION III - CERTIFICATION

7. CERTIFICATION OF REPORT BY CONTRACTOR/SUBCONTRACTOR (Not required if: (X as appropriate)) SMALL BUSINESS or NONPROFIT ORGANIZATION

I certify that the reporting party has procedures for prompt identification and timely disclosure of "Subject Inventions," that such procedures have been followed and that all "Subject Inventions" have been reported.

a. NAME OF AUTHORIZED CONTRACTOR/SUBCONTRACTOR OFFICIAL (Last, First, Middle Initial)	b. TITLE	c. SIGNATURE	d. DATE SIGNED
Mr. Michael A. Petrik	Vice President	*[signature]*	7-12-00

DD FORM 882, JAN 1999 (EG) PREVIOUS EDITION MAY BE USED.